

# Biomimetic Control of Myoelectric Prosthetic Hand Based on a Lambda-type Muscle Model

Akira Furui, Kosuke Nakagaki, and Toshio Tsuji

**Abstract**—Myoelectric prosthetic hands are intended to replace the function of the amputee’s lost arm. Therefore, developing robotic prosthetics that can mimic not only the appearance and functionality of humans but also characteristics unique to human movements is paramount. This paper proposes a novel biomimetic control method for myoelectric prosthetic hands integrating the impedance model with the concept of the  $\lambda$ -type muscle model. According to the state of the muscle, the proposed method can dynamically control the joint equilibrium position, and can maintain the joint angle naturally during muscle relaxation. The experimental results, based on comparison with the actual human joint angles, suggest that the proposed method has a better correlation with the actual human motion than the conventional methods. Additionally, the control experiments showed that the proposed method could achieve a natural prosthetic hand movement similar to that of a human, thereby allowing voluntary hand movements.

**Index Terms**— Prosthetics and exoskeletons, biomimetics, human-centered robotics.

## I. INTRODUCTION

A study published by the cabinet office of Japan reported more than 82,000 upper-limb amputations due to accidents or disease [1]. As a part of life support for upper-limb amputees, a myoelectric prosthetic hand is prescribed. The myoelectric prosthetic hand is controlled by inferring the amputee’s intentions from electromyogram (EMG), which is the electrical activity produced by muscles. As the myoelectric prosthetic hand can be manipulated voluntarily according to the exerted muscle force, there is a possibility that users would operate it as they use their hands.

Myoelectric prosthetic hands are designed to replace the lost arm and supplement the function of the upper limb. Thus, the prosthetic must realize human-like behavior mimicking the movements of the human hand in addition to its appearance and operability. However, most myoelectric prosthetic hands studied and developed thus far use a simple proportional control to open and close the hand in response to the muscle strength [2]–[6]. Therefore, human motion characteristics have not been sufficiently considered for these myoelectric prosthetic hands, and human-like behavior has not been realized entirely.

Studies on biomimetic control of prosthetic hands have focused on reflecting the human motion characteristics in the

prosthetic hand [7]–[9]. The authors previously introduced the impedance model-based biomimetic control method [10], [11] to control a prosthetic hand [8]. This model can realize natural human-like hand movements by controlling the actuators, considering the impedance parameters around the human joint. We showed that smooth movement according to the user’s EMG signals could be achieved through the experiments conducted on intact and amputee participants [8]. However, in the impedance control, the equilibrium angle at the resting state is fixed at the origin as the equilibrium position of the spring, and in consequence, the joint angle always converges to the origin, regardless of its position. In contrast, the actual human movement allows maintaining the joint angle during muscle relaxation after realizing the desired joint angle by muscle contraction. Therefore, the previously proposed impedance control is insufficient to replicate the characteristics of human movement.

In this regard, if we could develop a control system considering the movement characteristics of the muscles, it would be possible to control the equilibrium position of the joint angle dynamically, according to the contraction state of the muscles. Various theories have been proposed to model muscle dynamics [12]–[14]. Merton proposed the servo hypothesis ( $\gamma$ -model), assuming that the tonic stretch reflex is the primary motor control mechanism [12]. Bizzi *et al.* proposed an  $\alpha$ -model [13], relying on the hypothesis that the brain mainly controls the activity of  $\alpha$  motor neurons. Moreover, Feldman proposed the  $\lambda$ -model [14], assuming that the command from the central nervous system controls the threshold of the tonic stretch reflex. The  $\lambda$ -model is prone to be superior to other models in that it can explain the entire voluntary movement of humans to some extent in a concise theory [15]. Thus, the theory has been used as a major motion control theory for several decades.

This paper proposes a biomimetic control method for myoelectric prosthetic hands based on the impedance property of muscle and the concept of the  $\lambda$ -model. The proposed method can reflect human motor characteristics to the movement of the prosthetic hand by dynamically controlling the equilibrium angle of the joint according to the state of contraction/relaxation of the muscle.

## II. BIOMIMETIC CONTROL BASED ON THE $\lambda$ -TYPE MUSCLE MODEL

### A. Impedance Control Model

First, based on impedance control [11], the characteristics of joint motion are represented by the tension balance between flexors and extensors (Fig. 1). The equation of motion

Corresponding authors: Akira Furui and Toshio Tsuji.

A. Furui and T. Tsuji are with the Graduate School of Advanced Science and Engineering, Hiroshima University, Higashi-hiroshima, 739-8527 Japan (e-mail: akirafurui@hiroshima-u.ac.jp; tsuji@bsys.hiroshima-u.ac.jp)

K. Nakagaki is with the Graduate School of Engineering, Hiroshima University, Higashi-hiroshima, 739-8527 Japan (e-mail: nakagaki@bsys.hiroshima-u.ac.jp)

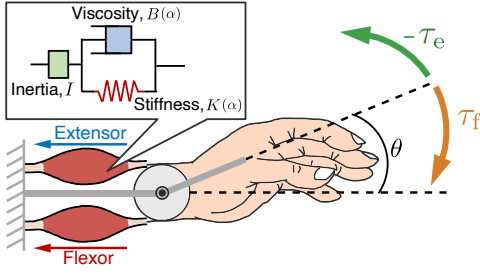


Fig. 1. Biomimetic impedance control based on the musculoskeletal model of the human joint. The characteristics of joint motion can be represented by the tension balance between flexors and extensors. By reflecting the impedance characteristics of human joints, natural and smooth control of the prosthetic hand can be achieved.

around each joint  $j$  ( $j = 1, 2, \dots, J$ ) of the prosthetic hand is defined as follows:

$$I_j \ddot{\theta}_j + B_j(\alpha_j) \dot{\theta}_j + K_j(\alpha_j)(\theta_j - \theta_j^0) = \tau_{jf} - \tau_{je}, \quad (1)$$

where  $I_j$ ,  $B_j(\alpha_j)$ , and  $K_j(\alpha_j)$  are the inertia, viscosity, and stiffness, respectively.  $\theta_j$  and  $\theta_j^0$  are the joint angle and its equilibrium angle of only the stiffness element. Furthermore,  $\tau_{jf}$  and  $\tau_{je}$  are the joint torque generated by the flexor and extensor, respectively. The change in the characteristics associated with muscle activity is expressed by defining the stiffness and viscosity as functions of the muscle contraction level  $\alpha_j$  ( $0 \leq \alpha_j \leq 1$ ).

$$K_j(\alpha_j) = k_{j,1} \alpha_j^{k_{j,2}} + k_{j,3}, \quad (2)$$

$$B_j(\alpha_j) = b_{j,1} \alpha_j^{b_{j,2}} + b_{j,3}, \quad (3)$$

The equilibrium angle  $\theta_j^{\text{eq}}$  of the complete system can be calculated as the joint angle  $\theta_j$  when  $\ddot{\theta}$  and  $\dot{\theta} = 0$ .

$$\theta_j^{\text{eq}} = \frac{1}{K_j(\alpha_j)} (\tau_{jf} - \tau_{je}) + \theta_j^0. \quad (4)$$

## B. Model Requirements

From (4), the torque  $\tau_j(t)$  and the equilibrium angle  $\theta_0$  of the joint angle can be adapted to control the equilibrium angle of the model dynamically, according to the muscle contraction state. This study designs these variables to build a control model satisfying the following specifications:

- **Specification 1:** When the muscle relaxes, the equilibrium position is maintained at the value just before relaxation.
- **Specification 2:** Continuity of the equilibrium position is maintained even when the direction of motion changes from flexion to extension or extension to flexion.

When designing the model, it is desirable to consider all muscle information for the joint movement. However, various muscles act when a person performs a complicated operation, such as flexing their fingers. Thus, it is difficult to estimate all the muscle information on the joint motion from the EMG signals. Therefore, we switch the muscle contraction level

depending on the classified motion as follows:

$$\alpha_j(t) = \begin{cases} \alpha_{jf}(t) & \text{(Flexion motion)} \\ \alpha_{je}(t) & \text{(Extension motion)} \end{cases}. \quad (5)$$

Furthermore, the torque  $\tau_{jf}$ ,  $\tau_{je}$  can be expressed as a function of the muscle contraction level  $\alpha(t)$ :

$$\tau_{ji}(t) = \alpha_{ji}(t) \tau_{ji}^{\text{max}}, \quad (6)$$

where  $\tau_{ji}^{\text{max}}$  is the maximum value of each predetermined torque, and the subscript  $i \in \{f, e\}$  indicates flexor and extensor. Henceforth, we omit  $(t)$  to indicate a function of time, except when highlighting the temporal context.

## C. Invariant Condition During Muscle Relaxation

We first design a model satisfying specification 1. In the model design, we adopt the concept of the  $\lambda$ -model [14], which is a model of human muscle movements. The  $\lambda$ -model assumes that the brain achieves the motion by controlling the muscle length  $x$ , while the intensity of the motor commands determines the threshold  $\lambda$  of the muscle length. Motion conditions of the muscle are formulated as follows:

$$x - \lambda > 0. \quad (7)$$

The muscle is active if the condition of (7) expression is satisfied; otherwise, the muscle activity is stopped, and the current state is maintained. The muscle activity level  $s$  in the  $\lambda$ -model is defined as a function of the muscle length  $x$  and threshold  $\lambda$ . We assume that  $s$  is a simple linear function that can be written as follows:

$$s = s(x, \lambda) = G(x - \lambda) + h, \quad (8)$$

where  $G$  and  $h$  are constants, and (8) can be rewritten as

$$x - \lambda = \frac{1}{G}(s - h). \quad (9)$$

Here, we assume that the constant  $G$  is the maximum value  $s^{\text{max}}$  of  $s$ , and  $s/G$  in (9) can be regarded as the muscle contraction level  $\alpha_{ji}$ . Furthermore, if the constant  $h/G$  is considered as the threshold value  $\tilde{\lambda}_{ji}$  of the muscle contraction level, from the conditional expression (7), the muscle length  $x$  can be replaced by the muscle contraction level  $\alpha_{ji}$ , and the muscle length threshold  $\lambda$  can be replaced by the muscle contraction level threshold  $\tilde{\lambda}_{ji}$ . Subsequently, the muscle activity condition in the control model is defined as follows:

$$\alpha_{ji} - \tilde{\lambda}_{ji} > 0. \quad (10)$$

Here, we introduce a function expressing the active state of the muscle using the activity condition (10) as follows:

$$C_i^+ = [\alpha_{ji} - \tilde{\lambda}_{ji}]^+ = \begin{cases} 1 & (\alpha_{ji} - \tilde{\lambda}_{ji} > 0) \\ 0 & (\alpha_{ji} - \tilde{\lambda}_{ji} \leq 0) \end{cases}, \quad (11)$$

$$C_i^- = 1 - C_i^+, \quad (12)$$

where  $C_i^+$  is a function expressing the active state of the muscle and becomes  $C_i^+ = 1$  when  $\alpha_{ji}$  is larger than the threshold  $\tilde{\lambda}_{ji}$ . Meanwhile,  $C_i^-$  expresses the inactive state

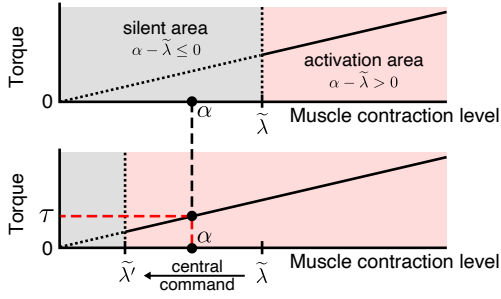


Fig. 2. Invariant condition during muscle relaxation based on the concept of the  $\lambda$ -model. The muscle contraction level threshold  $\tilde{\lambda}$  defines the silent and activation areas. The torque is generated only when the current muscle contraction level is in the activation area.

of the muscle and becomes  $C_i^- = 1$  when  $\alpha_{ji}$  is equal to or less than the threshold  $\tilde{\lambda}_{ji}$ . We consider that the joint angle varies when the muscular activity condition is satisfied, and it is maintained when the muscle is in an inactive state, according to the concept of the  $\lambda$ -model (Fig. 2). Then, using (11) and (12), we define  $\tau_{jf}$ ,  $\tau_{je}$ , and  $\theta_{ji}^0$  as follows:

$$\tau_{ji} = C_i^+ \tau_{ji}^{\max} \alpha_{ji}, \quad (13)$$

$$\theta_{ji}^0(t) = C_i^- \theta_{ji}^{\text{eq}}(t - \Delta t), \quad (14)$$

where  $\theta_{ji}^{\text{eq}}(t - \Delta t)$  is the equilibrium angle before the sampling time  $\Delta t$ .

Subsequently, we perform the control using muscle information only in the flexion or extension direction based on the constraint condition mentioned above. A separate model is defined for each direction, and control is achieved by switching between models. Under this condition, when a model is applied in a specific direction, the muscle contraction in the other direction is zero, which leads to the discontinuous torque and equilibrium position before and after switching the models if the control is based on (13) and (14). The continuity of the equilibrium position can be maintained by supplementing the muscle contraction level in the non-classified direction with the muscle contraction level in the classified direction. Based on this assumption, when the flexion direction is classified, the muscle contraction level  $\alpha_{je}$  in the extension direction is expressed as follows:

$$\alpha_{je} = A_e(1 - \alpha_{jf}), \quad (15)$$

where  $A_e$  is a constant. Here, substituting (15) into (13), the control model in the flexion direction is

$$\begin{cases} \tau_{jf} = C_f^+ \tau_{jf}^{\max} \alpha_{jf} \\ \tau_{je} = C_f^+ \tau_{je}^{\max} A_e(1 - \alpha_{jf}) \end{cases} \quad (\text{Flexion direction}). \quad (16)$$

Similarly, when the extension direction is classified, the muscle contraction level  $\alpha_{jf}$  in the flexion direction is expressed as

$$\alpha_{jf} = A_f(1 - \alpha_{je}), \quad (17)$$

where  $A_f$  is a constant. Thus, the control model in the extension direction is

$$\begin{cases} \tau_{jf} = C_e^+ \tau_{jf}^{\max} A_f(1 - \alpha_{je}) \\ \tau_{je} = C_e^+ \tau_{je}^{\max} \alpha_{je} \end{cases} \quad (\text{Extension direction}). \quad (18)$$

From the above equations, by considering the muscle activity condition based on the  $\lambda$ -model for muscle motion, we can construct a model that maintains the equilibrium position of the joint angle even when the muscle relaxes.

#### D. Continuity Condition when Switching Motion Direction

We next consider the continuity of the equilibrium position at the time of changing the model to satisfy specification 2. We consider that a model is applied in the extension direction at time  $t_e$  and then in the flexion direction at time  $t_e + \Delta t$ . At this time, the equation of motion of the model in the extension direction applied at  $t_e$  becomes

$$\begin{aligned} I_j \ddot{\theta}_j + B_j(\alpha_{je}(t_e)) \dot{\theta}_j + K_j(\alpha_{je}(t_e)) \theta_j \\ = \tau_{jf}^{\max} A_f(t_e)(1 - \alpha_{je}(t_e)) - \tau_{je}^{\max} \alpha_{je}(t_e). \end{aligned} \quad (19)$$

The equation of motion of the model in the flexion direction applied at  $t_e + \Delta t$  immediately thereafter is given as

$$\begin{aligned} I_j \ddot{\theta}_j + B_j(\alpha_{jf}(t_e + \Delta t)) \dot{\theta}_j + K_j(\alpha_{jf}(t_e + \Delta t)) \theta_j \\ = \tau_{jf}^{\max} \alpha_{jf}(t_e + \Delta t) \\ - \tau_{je}^{\max} A_e(t_e + \Delta t)(1 - \alpha_{jf}(t_e + \Delta t)). \end{aligned} \quad (20)$$

The equilibrium positions of (19) and (20) must be equal to maintain continuity at the time the model switches. Here, we assume that the state of motion is the steady state ( $\ddot{\theta}_j, \dot{\theta}_j = 0$ ) just before switching the direction of motion. The equilibrium positions in (19) and (20) are

$$\theta_j(t_e) = \frac{1}{K_j(\alpha_{je}(t_e))} \{ \tau_{jf}^{\max} A_f(t_e)(1 - \alpha_{je}(t_e)) - \tau_{je}^{\max} \alpha_{je}(t_e) \}, \quad (21)$$

$$\theta_j(t_e + \Delta t) = \frac{1}{K_j(\alpha_{jf}(t_e + \Delta t))} \{ \tau_{jf}^{\max} \alpha_{jf}(t_e + \Delta t) - \tau_{je}^{\max} A_e(t_e + \Delta t)(1 - \alpha_{jf}(t_e + \Delta t)) \}. \quad (22)$$

Solving the above equations for  $A_e$  and organizing it by substituting in equation (16), we obtain the following torque expressions when the flexion direction is determined.

$$\begin{cases} \tau_{jf} = C_f^+ \tau_{jf}^{\max} \alpha_{jf} \\ \tau_{je} = C_f^+ \frac{1 - \alpha_{jf}}{1 - \alpha_{jf}^{\text{post}}} (\tau_{jf}^{\max} \alpha_{jf}^{\text{post}} - K_j(\alpha_{jf}^{\text{post}}) \theta_{je}^{\text{pre}}) \end{cases}, \quad (23)$$

where  $\theta_{je}^{\text{pre}} = \theta_{je}(t_e)$  is the equilibrium angle just before switching, and  $\alpha_{jf}^{\text{post}} = \alpha_{jf}(t_e + \Delta t)$  is the muscle contraction level in the flexion direction immediately after switching. Similarly, when the model is applied in the flexion direction at time  $t_f$  and there is a switch to the model in the extension direction at time  $t_f + \Delta t$ , the torques  $\tau_{jf}$  and  $\tau_{je}$  in the extension direction can be written as follows:

$$\begin{cases} \tau_{jf} = C_e^+ \frac{1 - \alpha_{je}}{1 - \alpha_{je}^{\text{post}}} (\tau_{je}^{\max} \alpha_{je}^{\text{post}} + K_j(\alpha_{je}^{\text{post}}) \theta_{jf}^{\text{pre}}) \\ \tau_{je} = C_e^+ \tau_{je}^{\max} \alpha_{je} \end{cases}, \quad (24)$$

where  $\theta_{jf}^{\text{pre}} = \theta_{jf}(t_f)$  is the equilibrium angle just before switching, and  $\alpha_{je}^{\text{post}} = \alpha_{je}(t_f + \Delta t)$  is the muscle contraction level in the extension direction immediately after

switching. Finally, using (1), (23), and (24), the control model for the direction  $i \in \{f, e\}$  is obtained as follows:

$$I_j \ddot{\theta}_j(t) + B_j(\alpha_{ji}) \dot{\theta}_j(t) + K_j(\alpha_{ji})(\theta_j(t) - \theta_{ji}^0(t)) = C_i^+ \delta_i \tau_{ji}^{\max} (\alpha_{ji}(t) - V_i(t) \alpha_{ji}^{\text{post}}), \quad (25)$$

$$\theta_{ji}^0(t) = C_i^+ \frac{K_j(\alpha_{ji}^{\text{post}})}{K_j(\alpha_{ji})} V_i(t) \theta_{ji}^{\text{pre}} + C_i^- \theta_{ji}^{\text{eq}}(t - \Delta t), \quad (26)$$

where  $\delta_f = 1$ ,  $\delta_e = -1$ , and

$$V_i(t) = \frac{1 - \alpha_{ji}(t)}{1 - \alpha_{ji}^{\text{post}}}. \quad (27)$$

### III. EMG-BASED CONTROL EXPERIMENTS

#### A. Methods

To evaluate the applicability of the proposed method to the prosthetic hand control, we constructed a myoelectric prosthetic hand system and performed control experiments using EMG signals. All measurement experiments were approved by the Hiroshima University Ethics Committee (registration number E-840).

1) *Experimental System:* Fig. 3(a) shows an overview of the control system of the myoelectric prosthetic hand based on the proposed biomimetic control method. The system consists of three parts: EMG signal processing, prosthetic hand control, and a myoelectric prosthetic hand. The prosthetic hand movement can be controlled using a proportional-integral-derivative (PID) controller.

The EMG signal recording/processing and the prosthetic hand control were implemented in the electrical apparatus, which consists of EMG electrodes (OttoBock 13-E200, Otto Bock HealthCare), a microcomputer, and a motor driver (Fig. 3(b)). The exterior and other parts were printed using a three-dimensional printer. We designed the parts based on open-source models released by the Open Hand Project [16] and Open Bionics Ada Hand [17]. Each finger has a wire that is wound around a spool (Fig. 3(c)). Subsequently, an actuator based on a DC motor rotates the spool so that the finger flexes (Fig. 3(d)). For more detailed information on hardware structure, please refer to [8].

The EMG signal processing involved feature extraction and motion classification. Feature extraction for the measured EMG signals from the  $L$  electrodes was conducted according to the method used in [8], in which the measured EMG signals are rectified, smoothed, and normalized to make the sum of all the channels equal to 1.0. Furthermore, the normalized EMG signal was averaged over all channels to calculate the force information  $F_{\text{EMG}}(t)$ . Motion was recognized when  $F_{\text{EMG}}(t)$  was greater than a threshold  $F^{\text{th}}$ . Let  $m_f$  and  $m_e$  be movements in the flexion and extension directions, respectively, the muscle contraction level in the respective motion directions are defined as follows:

$$\alpha_i(t) = \frac{F_{\text{EMG}}(t)}{F_{m_i=m_i'}^{\max}} \quad (i \in \{f, e\}), \quad (28)$$

where  $F_{m_i}^{\max}$  is  $F_{\text{EMG}}(t)$  at the maximum muscle contraction with respect to each motion  $m_i \in \{1, 2, \dots, M\}$  ( $M$  is the

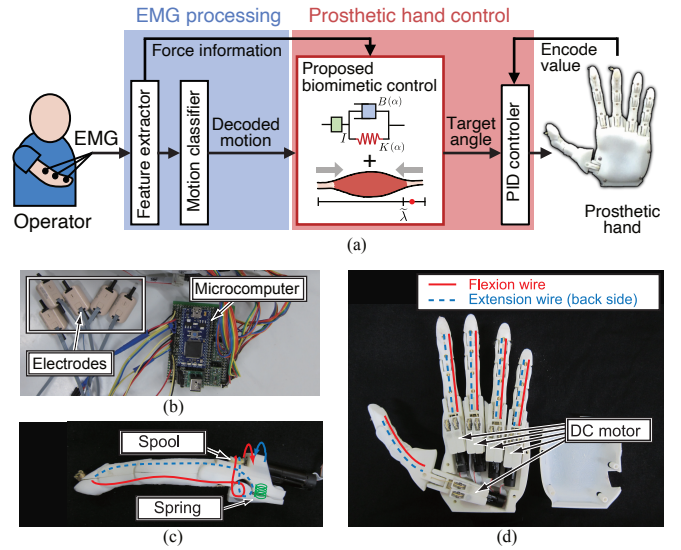


Fig. 3. Overview of the experimental prosthetic hand system. (a) Based on the measured EMG signals, the force information and EMG feature patterns are calculated. The operator's motions are subsequently decoded from the EMG patterns, and the joint angle of the prosthetic hand is calculated using the proposed control method. The prosthetic hand movement can then be performed using a PID controller. (b–d) The hardware configuration.

number of motions) measured in advance. By treating  $\alpha_i(t)$  as the muscle contraction level in the control model, we realize EMG-based voluntary control of the motor angles. The motion classification uses a recurrent log-linearized Gaussian mixture network (R-LLGMN) [18], a recurrent neural network comprising a Gaussian mixture model and a hidden Markov model, thereby considering the time-series characteristics of the operator's motions. The system handles movements in the flexion and extension directions of each motion as a separate class; hence, the number of classes learned and classified by the R-LLGMN is  $M \times 2$ .

2) *Evaluation of the Joint Angle Calculation:* An experiment was conducted on the joint angle calculation for the flexion and extension motion of the wrist to verify the effectiveness of the proposed method. In the experiment, five healthy male participants (aged 23–25 years) adopted a posture with their forearm on a desk and their palm vertical while sitting. A cushioning material was placed between the wrist joint and the desk to prevent friction with the desk. The EMG signals were measured using two sensors ( $L = 2$ ) attached to the flexor carpi radialis and the extensor carpi radialis longus muscles. Simultaneously, the joint angle of the wrist was measured by a goniometer (SG65, Biometrix), attached from the third metacarpal bone of the back of the hand to the midline of the forearm. The sampling frequency of the EMG sensors and goniometer was set to 500 Hz. The experiments considered only the wrist motion ( $M = 1$ ), and the classes learned and classified using the R-LLGMN were set to two classes of wrist flexion and extension.

First, the R-LLGMN was trained for each participant. They were instructed to flex and then extend the wrist, and the corresponding EMG signals were acquired. We randomly selected 100 samples from each of the EMG patterns for flexion and extension and used them as the training data.

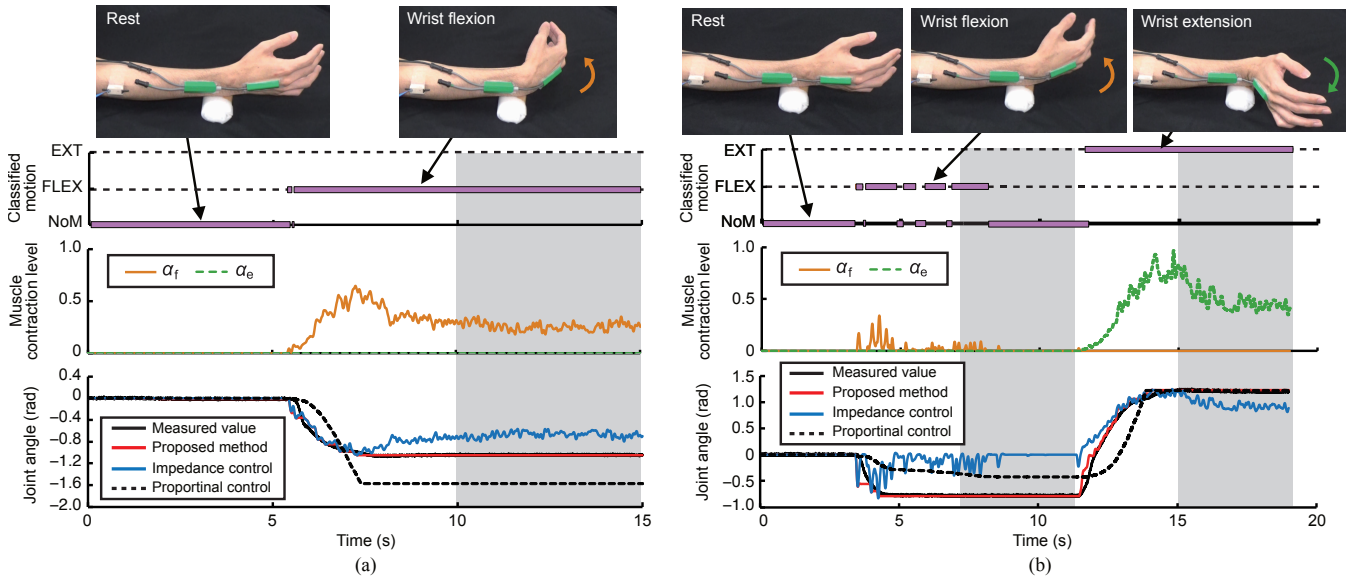


Fig. 4. Examples of the measured muscle contraction level and estimated angles. (a) Task 1. (b) Task 2. The shaded areas represent the sections of muscle relaxation. The motions conducted by the participants were no motion (NoM), wrist flexion (FLEX), and wrist extension (EXT).

The participants then performed the flexion and extension of the wrist joint while following a target joint angle, which was presented on the screen. The joint angles of the participants were also shown to them in real-time in the form of a line graph. In the experiment, three trials were performed for each of the two tasks. Task 1 comprised an initial rest (5 s), wrist flexion of  $\pi/3$  rad (5 s), and remain in the same position with muscle relaxation (5 s). Task 2 comprised an initial rest (3 s), wrist flexion of  $\pi/4$  rad (4 s), remain with muscle relaxation (4 s), wrist extension of  $7\pi/18$  rad (4 s), and remain with muscle relaxation (4 s). The state where the forearm and palm were horizontal is assumed to be the initial state (0 rad). During each task, the joint angle was estimated by the proposed method based on the muscle contraction level  $\alpha_i$  and the decoded motion by R-LLGMN. In the experiment, the number of components in the R-LLGMN was set to 1, the threshold was set to  $F^{\text{th}} = 0.02$ , and the cut-off frequency of signal filtering was set to 8.0 Hz. The impedance parameters were set to the values of the wrist joint based on a previous study [11].

We compared the estimated joint angle and the actual joint angle measured by the goniometer to verify the accuracy. The root-mean-square error (RMSE) between the measured and the estimated angles was calculated at every time point as an index of the estimation accuracy for the joint angle. For comparison, the joint angles were similarly obtained using a conventional impedance control method [11] and proportional control method [2], and the RMSE was also calculated. In the proportional control method, the estimated joint angle range was limited to  $[-\pi/2, 7\pi/18]$ , which corresponded to the motion range of the wrist joint.

3) *Prosthetic Hand Control*: Control experiments of a myoelectric prosthetic hand were performed using a prosthetic hand system and the proposed control method. The participant was a healthy male (aged 24 years), and the electrode placement and performed movements were the same

as in the previous experiment. In this experiment, the flexion and extension of the wrist corresponded to the grasping and opening motions of the prosthetic hand, respectively. The participant performed flexion and extension of the wrist, in turn, with a muscle relaxation period between each motion. The D component of the PID control was omitted, and the control cycle of the microcomputer was 5 ms. The impedance parameters used were those of the human finger joints [11].

## B. Results

Fig. 4 shows examples of joint angle calculation for each task. The upper, middle, and lower panels represent the classified motions, muscle contraction levels, and joint angles, respectively. The shaded area in the figure corresponds to the section where the participants were instructed to relax. Fig. 5 shows the average RMSE over participants for each task. The statistical test results of a paired  $t$ -test (significance level of 5%) with Holm adjustment are also shown.

Fig. 6 shows the control experiment results. The upper, middle, and lower panels represent the classified motions, muscle contraction levels, and motor output angles, respectively. The opening motion of the prosthetic hand was set as the initial state, implying that the initial angle was zero. Shaded areas represent sections of muscle relaxation.

## C. Discussion

In the joint angle calculation experiment, the RMSE was used to evaluate the error between the actual human joint angle and the estimated joint angle based on the control models, using muscle contraction information. The RMSE of the proposed method was smaller than that of the other methods in both tasks, suggesting that the proposed method can realize more human-like wrist motions with relatively high accuracy. Although this tendency was similar for all sections, it was more remarkable in the relaxation section.

In the conventional impedance control method, as the origin of the joint angle is permanently fixed to the initial

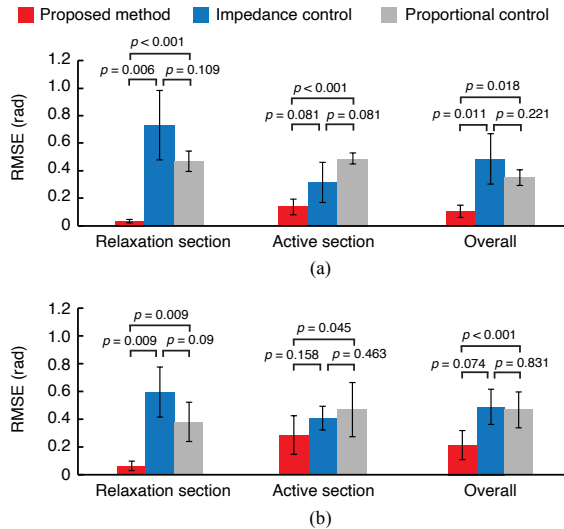


Fig. 5. Root-mean-square error (RMSE) for relaxation section, active section, and overall. (a) Taks 1. (b) Task 2. Error bars represent the standard deviations of all participants.  $p$  values obtained by paired  $t$ -test with Holm adjustment are also presented.

position, the equilibrium and joint angles converge to the initial position when the muscle is relaxed. Therefore, the error of the impedance control method is higher in the section where the wrist joint angle is maintained in the muscle relaxation. The proportional control method showed lower RMSEs than the impedance control method in the muscle relaxation section because of the angle saturation in the proportional control method. However, this method cannot calculate the joint angle by considering the movement characteristics of a human, resulting in errors in the transition process of the joint angle. In contrast, the proposed method could maintain the equilibrium angle based on the muscle model, resulting in a relatively small error in the joint angle estimation. Moreover, as the control model involved the impedance characteristics of the human, the human-like smoothness was replicated when changing the joint angle; hence, the error during the transition was small. These results suggest the effectiveness of the proposed method to dynamically control the equilibrium position, even during muscle relaxation, in reproducing human joint movements.

Furthermore, we verified the applicability of the proposed control method through an experiment considering prosthetic hand control. In Fig. 6, the joint angle of the prosthetic hand is smoothly controlled according to the operator's movements. We can also confirm that the motor angle is maintained during muscle relaxation by dynamically changing the equilibrium position. Therefore, through the proposed control method, the state of the muscle, such as contraction or relaxation, was reflected in the motion of the prosthetic hand; thus, the human motion characteristics could be reproduced.

In the conventional impedance control method, maintaining the muscles contracted through invariance of the equilibrium angle is necessary to keep the joint angle, which may increase the burden on the user. The EMG signal pattern change due to muscle fatigue when the muscles are

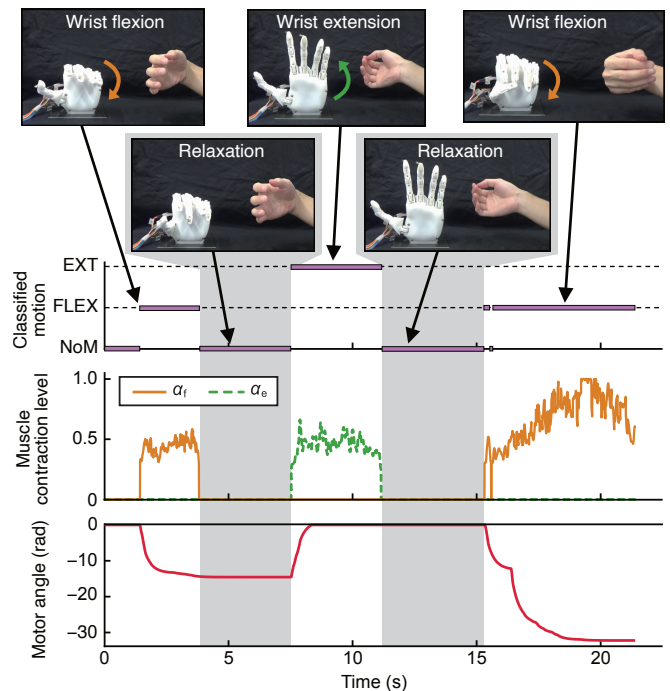


Fig. 6. Results of the prosthetic hand control experiment. The shaded areas represent the sections of muscle relaxation. The participants performed no motion (NoM), wrist flexion (FLEX), and wrist extension (EXT). The wrist flexion and extension of the participant corresponded to the hand closing and opening of the prosthetic hand.

contracted for a long time, thereby affecting the operability of myoelectric prosthetic hands [19], [20]. In contrast, the proposed method dynamically controls the equilibrium angle and can maintain the motion even when the muscles relax. Therefore, the proposed method has the potential to reduce muscle fatigue and improve the operability of prosthetic hands during long-term use.

One of the limitations of this study includes the limited number of participants. To generalize the findings of this study, we will increase the number of participants, including amputees, and conduct further investigation in the future.

#### IV. CONCLUSIONS

This paper proposed a biomimetic control method based on the  $\lambda$ -model, which is a muscle motion model. The proposed method is capable of controlling the equilibrium angle of a joint dynamically and continuously according to the state of a muscle. Moreover, it is possible to realize a smooth motion based on the impedance characteristics of a person.

The joint angle calculation experiments revealed that the proposed method outperforms the conventional control method in terms of matching actual joint angle changes. Moreover, the proposed method was introduced into the control system of a prosthetic hand, and the control experiment was conducted by a non-amputee participant. The results suggested that a prosthetic hand movement similar to human behavior could be realized through the proposed method, which would lead to the reduction of muscle fatigue during long-term use.

## REFERENCES

- [1] “Annual report on government measures for persons with disabilities,” Cabinet Office, Government of Japan, Tech. Rep., 2013.
- [2] “OttoBock,” Accessed on Sep. 24, 2020. [Online]. Available: <http://www.ottobock.com/>
- [3] “Vincent systems,” Accessed on Sep. 24, 2020. [Online]. Available: <https://vincentsystems.de/en/>
- [4] P. Parker, K. Englehart, and B. Hudgins, “Myoelectric signal processing for control of powered limb prostheses,” *J. Electromyogr. Kinesiol.*, vol. 16, no. 6, pp. 541–548, Dec. 2006.
- [5] M. Atzori and H. Müller, “Control capabilities of myoelectric robotic prostheses by hand amputees: A scientific research and market overview,” *Front. Syst. Neurosci.*, vol. 9, pp. 1–7, Nov. 2015.
- [6] N. Wang, K. Lao, and X. Zhang, “Design and myoelectric control of an anthropomorphic prosthetic hand,” *J. Bionic Eng.*, vol. 14, no. 1, pp. 47–59, Jan. 2017.
- [7] N. M. Kakoty, S. M. Hazarika, M. H. Koul, and S. K. Saha, “Model predictive control for finger joint trajectory of TU biomimetic hand,” in *Proc. IEEE Int. Conf. Mechatron. Autom.*, Aug. 2014, pp. 1225–1230.
- [8] A. Furuji, S. Eto, K. Nakagaki, K. Shimada, G. Nakamura, A. Masuda, T. Chin, and T. Tsuji, “A myoelectric prosthetic hand with muscle synergy-based motion determination and impedance model-based biomimetic control,” *Sci. Robot.*, vol. 4, no. 31, eaaw6339, June 2019.
- [9] M. Laffranchi, *et al.*, “The hannes hand prosthesis replicates the key biological properties of the human hand,” *Sci. Robot.*, vol. 5, no. 46, eabb0467, Sept. 2020.
- [10] T. Tsuj, O. Fukuda, H. Shigeyoshi, and M. Kaneko, “Bio-mimetic impedance control of an EMG-controlled prosthetic hand,” in *Proc. IEEE/RJS Int. Conf. Intell. Robots Syst.*, vol. 1, Oct. 2000, pp. 377–382.
- [11] T. Tsuji, K. Shima, N. Bu, and O. Fukuda, “Biomimetic impedance control of an EMG-based robotic hand,” in *Robot Manipulators*, A. Jimenez, Ed. InTech, Mar. 2010, ch. 9, pp. 213–231.
- [12] P. A. Merton, “Speculations on the servo-control of movement,” in *Ciba Foundation Symposium - The Spinal Cord*, ser. Novartis Foundation Symposia, G. E. W. Wolstenholme, Ed. Chichester, UK: John Wiley & Sons, Ltd., 1953, vol. 83, pp. 247–260.
- [13] E. Bizzi, W. Chapple, and N. Hogan, “Mechanical properties of muscles: Implications for motor control,” *Trends Neurosci.*, vol. 5, pp. 395–398, Jan. 1982.
- [14] A. G. Feldman, “Once more on the equilibrium-point hypothesis (lambda model) for motor control,” *J. Mot. Behav.*, vol. 18, no. 1, pp. 17–54, Mar. 1986.
- [15] M. L. Latash, M. F. Levin, J. P. Scholz, and G. Schöner, “Motor control theories and their applications,” *Medicina*, vol. 46, no. 6, pp. 382–392, 2010.
- [16] “Open hand project web page,” Accessed on: Sep. 24, 2020. [Online]. Available: <http://www.openhandproject.org/>
- [17] “OpenBionics web page,” Accessed on: Sep. 24, 2020. [Online]. Available: <http://openbionics.org>
- [18] T. Tsuji, Nan Bu, O. Fukuda, and M. Kaneko, “A recurrent log-linearized Gaussian mixture network,” *IEEE Trans. Neural Netw.*, vol. 14, no. 2, pp. 304–316, Mar. 2003.
- [19] M. Asghari Oskoei and H. Hu, “Myoelectric control systems—a survey,” *Biomed. Signal Process. Control*, vol. 2, no. 4, pp. 275–294, Oct. 2007.
- [20] D. Yang, Y. Gu, N. V. Thakor, and H. Liu, “Improving the functionality, robustness, and adaptability of myoelectric control for dexterous motion restoration,” *Exp. Brain Res.*, vol. 237, no. 2, pp. 291–311, Feb. 2019.